J Therm Anal Calorim (2014) 115:1359–1369
DOI 10.1007/s10973-013-3464-x

Thermoanalytical study of acid-treated clay containing amino acid immobilized on its surface

P. Rangel-Rivera · G. Rangel-Porras · H. Pfeiffer-Perea · E. Lima-Muñoz

Received: 17 June 2013 / Accepted: 4 October 2013 / Published online: 19 November 2013

Abstract The aim of this study is to investigate the incorporation of amino acid molecules in an acid-activated montmorillonite by means of solid characterization after the incorporation of these biomolecules. The acid activation procedure was carried out for the purpose of increasing the acid sites in the clay as well as the impurity elimination in the mineral. Cysteine, aspartic, and glutamic acids were adsorbed on montmorillonite K10 which was previously treated with a hydrochloric acid solution. The clay was put in contact with amino acid solutions at two different concentrations. Each amino acid was adsorbed at identical conditions, with the pH fixed to ensure the charge of molecules and surface clay. The solid was characterized by means of X-ray diffraction, infrared spectroscopy, thermogravimetric analysis, and nitrogen adsorption at 77 K. After the amino acid adsorption, the powders showed changes in their characteristics as well as in their thermal behavior, which depended on both the concentration and the nature of the adsorbed amino acid. The thermal decomposition and elimination of cysteine occurred at a higher temperature than the aspartic and glutamic acid; the complete removal of glutamic acid molecules was not observed at 850 °C. The differences observed in the solid characteristic after the adsorption of each amino acid were discussed. Both the thermoanalytical study and characterization of materials after the interaction with amino acid molecules can be useful to understand the adsorption mechanism of biomolecules on solid surfaces.

Keywords Thermogravimetric analysis · Clay · Amino acids · Adsorption · Characterization

P. Rangel-Rivera · G. Rangel-Porras (✉)
Department of Chemistry, University of Guanajuato, Noria Alta s/n, Col. Noria Alta, 36050 Guanajuato, GTO, Mexico
e-mail: gporras@ugto.mx; rangel_porrasgustavo@hotmail.com

H. Pfeiffer-Perea · E. Lima-Muñoz
Instituto de Investigación en Materiales, Universidad Nacional Autónoma de Mexico, Ciudad Universitaria, 04510 México, DF, Mexico

Introduction

The adsorption of amino acids on the surface of inorganic oxides has been the object of many experimental studies [1–5] and has attracted much interest in a wide range of fields such as medicine, aqueous geochemistry, soil science, technologies for the separation, and purification of biomolecules, and theories about the origins of life. For example, the case of these substance and other biological molecules interacting with metals or metal oxides such as TiO_2 has been of great interest because this interaction plays an important role in determining the biocompatibility of materials for their application as prostheses [6]. Environmental and geochemical studies of the interaction of amino acids with minerals have been carried out for the purpose of studying the distributions in marine sediments and soils of these biogenic organic compounds produced during organic matter decomposition [7, 8]. Immobilization of amino acid on clay is also suggested as one alternative for preparing organoclays which have applications as pollutant adsorbents, rheological control agents, paints, cosmetics, refractory varnish among others [9–11]. Furthermore, the adsorption of these molecules in powder as layered double hydroxides could be useful for polymerization in the new peptide synthesis [12, 13]. It has also been suggested that minerals could play an important role in the origin of life on earth, because they participate in the concentration of biomolecules from dilute solutions as well

as in the formation of biopolymers; consequently, several experiments have been carried out to test this hypothesis. Several good reviews related to the adsorption of amino acids on minerals appear in the literature [4, 5, 14–16]; among them, clays exhibit several useful properties that promote the adsorption of biomolecules, including high surface area and cationic exchange capacity, catalytic properties, intercalation of molecules in interlayer space, and global distribution. Most of the clay studied for adsorbing amino acids is smectite, particularly the montmorillonite type [5, 10, 11]. Many mechanisms have been suggested to account for the adsorption of biomolecules on clay, such as electrostatic interaction, ion exchange, or even weak interaction (Van der Waals forces). Nevertheless, the type of interaction that takes place between amino acids and clays is uncertain [17].

Montmorillonite is a mineral belonging to the smectite clay group, with two tetrahedral sheets of silica sandwiching a central octahedral sheet of alumina. The interlayer of montmorillonite is negatively charged owing to the substitution of magnesium(II) and sometimes iron(II) for aluminum(III), and has high cation-exchange capacity because of its structural nature and high surface area [18]. Montmorillonite also has proton adsorption/desorption site on its edge (aluminol and silanol groups). Therefore, the adsorption of amino acids on montmorillonite is expected to be mainly driven by electrostatic interaction between the negatively charged montmorillonite (with the interlayer and/or at the edge) and positively charged state of the amino acid. The interlayer has a structural charge originated from isomorphous substitutions within the montmorillonite structure. Therefore, the adsorptive properties of these materials are determined by its chemical composition, exchangeable ions, arrangement of crystalline structure, and particle agglomeration [19]. In consequence, among the main problems for studying, the immobilization of biomolecules in any mineral is the nonspecific composition of the material, which can vary according to the mineral deposit. In recent years, many studies have focused on understanding and enhancing the adsorption and catalytic processes carried out on the surface of these clays [20]. Acid activation of smectite, i.e., their partial dissolution in inorganic acids, is a common procedure to produce adsorbents [10, 21, 22]; in addition, the acid treatment is usually intended for a total dissolution of undesired nonclay components and particularly for a controlled attack on the octahedral layer in order to produce a more acidic Si-rich phase.

Amino acids consist of a basic amino group, an acidic carboxyl group, and a characteristic side chain. Depending on the degree of protonation of these functional groups ($NH_2 \leftrightarrow NH_3^+$, $COOH \leftrightarrow COO^-$), the net charge of an amino acid molecule changes greatly from positive or neutral to negative in an aqueous solution. Therefore, amino acids show various adsorption behaviors on materials, including electrostatic attraction, covalent bonding, hydrogen bonding, and hydrophobic interactions, which depend on environment conditions. Therefore, the respective charge of both the solid surface and the amino acid aliphatic group (R group) is apparently the main characteristic that determines the adsorption of these molecules. In this sense, minerals adsorb much more amino acid with a negatively or positively charged R group [5]. Once the amino acid is incorporated into the clay, its hydrothermal stability and reactivity are also behaved differently because of the interaction of its molecules with the solid, where the mineral characteristics can likewise be altered. Thus, the characterization of the solid after contact with a biomolecule solution has been useful to understand the interaction of these organic compounds with the clay. For example, X-ray diffraction analysis has made it possible to measure the distance between the montmorillonite 2:1 layers which reflection is observed between 2 and 10° of 2θ, and thus to know the presence of the amino acid molecule as well as its orientation in the interlayer space. On the other hand, infrared analyses serve to determine the protonation state of the amino acid functional group (i.e., $–NH_2$ vs. $–NH_3^+$, or $–COO^-$ vs. –COOH), thus providing information on the interaction between the solid surface and the organic molecule [23]. Finally, it is known that the adsorption capacity of a solid is limited by characteristics such as surface area and porosity [24]. A material with a high surface area and mesopores can be a good adsorbent of many chemical species where its capacity depends only on the nature of the adsorption sites. In this sense, there is commercial clay that provides solids with these characteristics. The present study aims to understand the adsorption of amino acids, such as aspartic acid, glutamic acid, and cysteine on acid-treated montmorillonite by means of thermogravimetric analysis, supported by additional methods for the characterization of materials such as X-ray diffraction, infrared spectroscopy, and adsorption of nitrogen at 77 K.

Materials and methods

Materials

The reagents used in this study were supplied by Sigma-Aldrich Company. The clay used for the adsorption tests consisted of montmorillonite K10 with a reported chemical composition of SiO_2 (73.0 %), Al_2O_3 (14.0 %), Fe_2O_3 (2.7 %), CaO (0.2 %), MgO (1.1 %), Na_2O (0.6 %), and K_2O (1.9 %). The amino acids used were aspartic acid, glutamic acid, and cysteine, which were used without further purification.

Prior to the adsorption study, the montmorillonite K10 was activated through acid treatment according to the following procedure: the solid in powder was suspended in a solution of hydrochloric acid 6 M at a rate of 8 mg of solid mL^{-1} of acid solution. The suspension was vigorously stirred for 24 h at room temperature. Then, the solid was recovered by centrifugation and washed three times with deionized water. After each washing, the powder was separated from the liquid by centrifugation. Finally, the acid-treated K10 was dried at 60 °C for 24 h.

Preparation of amino acid/K10 samples

The acid-treated K10 was impregnated with three amino acids: aspartic acid, glutamic acid, and cysteine. The procedure was carried out using an aqueous solution of organic molecules at two different concentrations for each amino acid, which were dissolved in a solution of sodium nitrate 0.01 M at a rate of 1 mmol of amino acid L^{-1} of solution (low concentration) and 100 mmol of amino acid L^{-1} of solution (high concentration). According with Mallakpour and Dinari [11], a cationic-exchange reaction was supposed to choose the concentration values. The solution of 1 mmol L^{-1} was very low concentration that all exchange sites could not be covered; while, 100 mmol L^{-1} was very high concentration that all these sites could be covered as well as others adsorption sites. The pH was set at 4.5 with nitric acid and sodium hydroxide. The amino acid solution was put in contact with acid-treated clay at a rate of 10 mg of clay mL^{-1} of amino acid solution. The suspension of clay–amino acid solution was stirred with a rotary movement of 150 rpm for 1 h at room temperature. Then, the powder containing the amino acid was separated from the liquid by centrifugation and washed three times with deionized water. After each washing, the powder was again separated from liquid by centrifugation. Finally, samples containing the amino acid were dried at 50 °C for 24 h. With the above procedure, six samples were obtained for studying: acid-treated K10 containing aspartic acid at two concentrations, one from the solution of 1 mmol L^{-1} and other from the solution of 100 mmol L^{-1}, which were called K10-Asp-1 and K10-Asp-100 respectively; similarly, the samples containing glutamic acid and cysteine were called K10-Glu-1, K10-Glu-100, K10-Cys-1, and K10-Cys-100.

The centrifugation for separating the solid from the liquid for the K10 activation and adsorption tests, were carried out with a Solbat centrifuge C-600, operating at 3,500 rpm for 15 min at room temperature.

Characterization of samples

X-ray diffractions (XRD) were carried out at room temperature on an Inel-Equinox diffractometer, having CuK_α radiation (1.54 Å). The diffraction patterns were collected between 2θ of 2° and 80°. The specimens were prepared by packing the samples powder in a glass holds. The XRD line profile analysis of peak was made with WINFIT computer program. The fitting parameters were refined by the classical Levenberg–Marquardt method. The d-spacing was calculated by using Bragg's equation ($n\lambda = 2d\sin\theta$). X-ray patterns of samples containing amino acids are only shown in the range of 2°–15° of 2θ for a better analysis of the $d(001)$ reflection.

Fourier transform infrared (FTIR) absorption spectra of sample powders were recorded on a Perkin-Elmer Spectrum 100, using KBr method in the range of 4,000–400 cm^{-1}. The samples for the KBr disk method were prepared by grinding a mixture of the solids and KBr powders in an agate mortar and pressing them in transparent disk. FTIR spectra of samples containing amino acids are only shown in the range from 1,200 to 1,800 cm^{-1} for a better analysis of organic group vibrations.

Nitrogen adsorption isotherm at 77 K was carried out on a Micromeritics apparatus ASAP-2010. The surface area was calculated by BET equation and the pore size distribution by BJH method. The samples were kept under vacuum pressure of 500 μmHg at 200 °C prior to their characterization in order to eliminate gas molecules from their surface and pores.

Thermogravimetric/derivative thermogravimetry (TG/DTG) analyses, in the range of 30–850 °C, were carried out on thermal Analyzer SDT-2960 TA instrument under a flow of air and a heating rate of 10 °C min^{-1}.

Results and discussions

Characterization of the acid-treated montmorillonite

K10 clay is a commercial montmorillonite used as adsorbent and catalysis. The main characteristic is a solid with a high surface area and mesoporous structure. The surface of this clay contains both the Brønsted and Lewis acid sites. The K10 clay was modified by means of acid treatment with the purpose of increasing the amount of acidic site in the solid as well as the dissolution of undesired nonclay components such as metallic species. The amount of acidic sites was measured by acid–base titration (Boehm method) [25, 26]. The amount of acidic sites in the untreated K10 was of 1.18 meq g^{-1} and in the acid-activated K10 was of 3.67 meq g^{-1}. XRD pattern showed similar reflection in both the samples in the range from 10° to 80° of 2θ, indicating that no considerable changes in the structure of the solid were induced after the acid treatment (Fig. 1). Nevertheless, the XRD patterns of acid-activated K10 depicted a broad peak from 3° to 8° of 2θ with a maximum

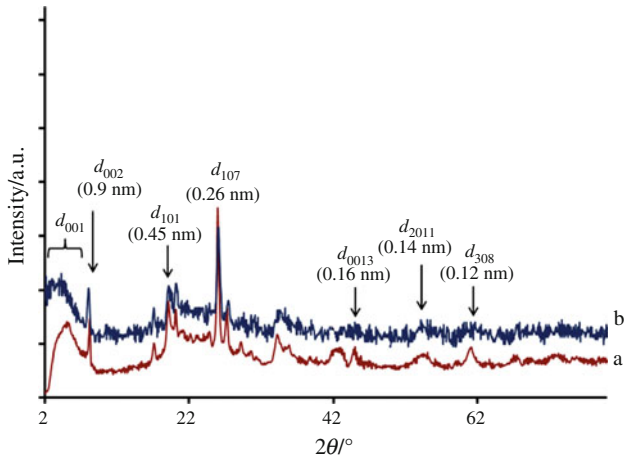

Fig. 1 X-ray diffraction patterns of **a** untreated K10 and **b** acid-treated K10

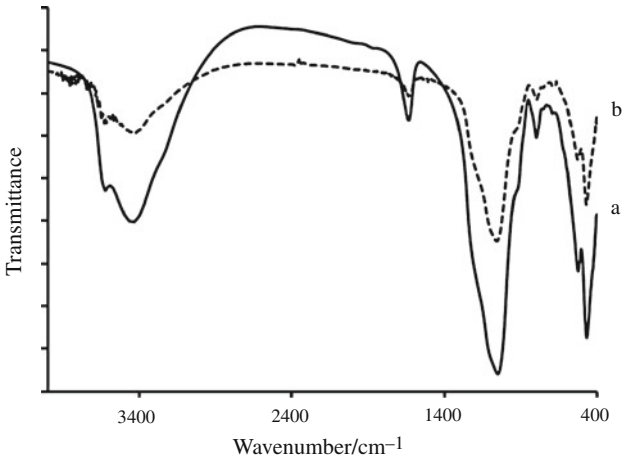

Fig. 2 FTIR spectra of *a* untreated K10 and *b* acid-treated K10

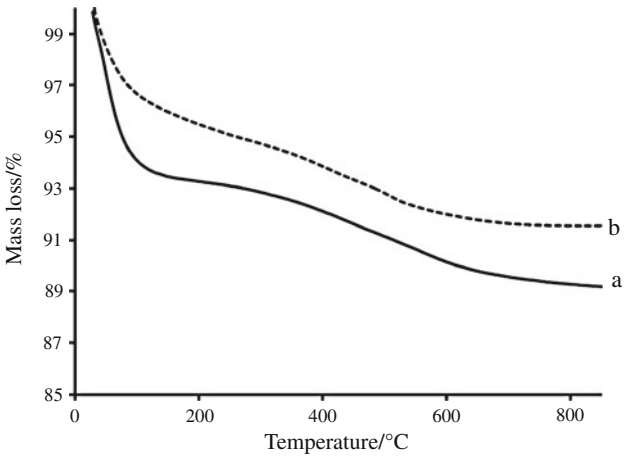

Fig. 3 Thermogravimetric analysis of **a** untreated K10 and **b** acid-treated K10

at 4.9°, which corresponded to *d*-spacing of 1.8 nm; meanwhile the untreated K10 showed a maximum at 5.2° that corresponding to *d*-spacing of 1.6 nm. The montmorillonite structure was swelled after the acid treatment with HCl, producing an increase in the interlayer space as well as the presence of broad peak in this range, which was associated to a heterogeneous arrangement of clay layers [27, 28].

Figure 2 shows infrared spectra of untreated and acid-treated montmorillonite. Similar spectra were obtained in both cases, indicating that the acid treatment did not produced considerable changes in the mineral structure. The adsorption band at 3,620 cm^{-1}, observed in montmorillonite spectra, is typical for smectites with high amount of Al in the octahedral. This peak is related to stretching vibration of OH groups. The broad band near 3,450 cm^{-1} is assigned to H–O–H vibrations of adsorbed water. The bending vibration of water molecules adsorbed on clay is observed at 1,640 cm^{-1}. Spectra show an intensive band at 1,030 cm^{-1} attributed to the Si–O stretching vibration, and at 530 and 470 cm^{-1} assigned to Si–O–Al (octahedral Al) and Si–O–Si bending vibrations, respectively. The OH bending bands appear at 914 cm^{-1} (Al_2OH) and 810 cm^{-1} (AlMgOH) [29].

The thermogravimetric analysis of acid-treated K10 revealed that mass loss was carried out in several stages at different temperatures (Fig. 3). The mayor mass loss of K10 clay occurred between 30 and 100 °C (3.4 %), which was due to water release for molecules weakly bonded to both the outer and inner surfaces of clay particles. The molecules strongly bonded to the interlayer cations required a temperature near 200 °C where mass loss of 4.5 % was reached. The second step was observed from 200 to 500 °C, accompanied by a mass loss of 2.7 % caused by the loss of bound water into either the layer space or interparticle water. In this temperature range, the DTG curve showed two maxima at 232 and 405 °C (Fig. 9). According to some authors, the dehydroxylation process in montmorillonite can take place before 500 °C is reached, depending on exchanged cations, surface vacancies, and structural parameters among other things [30, 31]; therefore, dehydroxylation reactions occurring in this range of heating were also suggested. A gradual mass loss was observed from 500 °C until 800 °C, which corresponded to 1.27 % of the mass of the initial solid. Dehydroxylation processes took place in the clay surface in this temperature range where new phases can be yield [32]. The untreated montmorillonite showed similar TG curve, but the mass loss in each step was higher than the observed after the acid treatment. The mass loss in untreated K10 was of 5.9 % (30–100 °C), 6.74 % (30–200 °C), 2.14 % (200–500 °C), and 1.85 % (500–800 °C). The decrease in the mass loss after the acid treatment of the mineral can due to that metallic ions were released during the acid procedure;

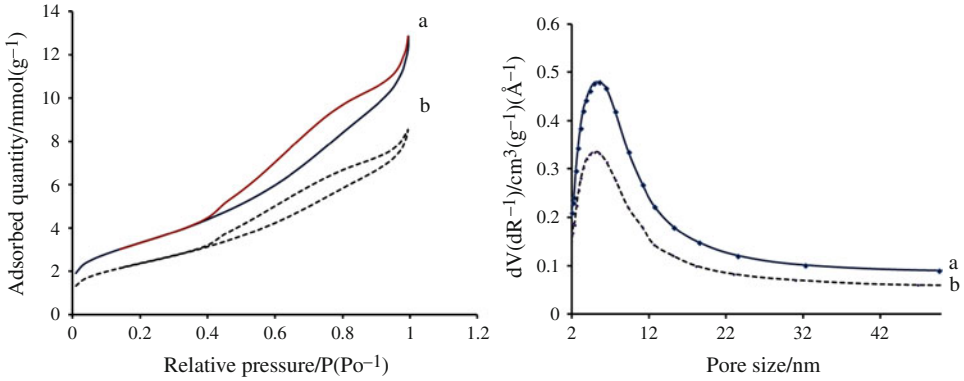

Fig. 4 Isotherm of nitrogen adsorption–desorption at 77 K (*left*) and BJH pore size distribution (*right*) of **a** untreated K10 and **b** acid-treated K10

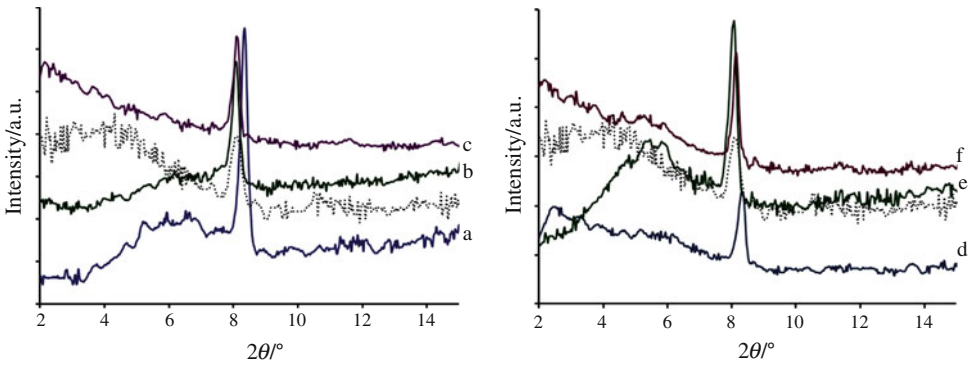

Fig. 5 X-ray diffraction patterns of K10 containing amino acids. *a* K10-Asp-1. *b* K10-Glu-1. *c* K10-Cys-1. *d* K10-Asp-100. *e* K10-Glu-100. *f* K10-Cys-100. The *dotted line* corresponds to acid-activated K10

therefore, less amount of water was coordinated with these metallic species [31].

The nitrogen adsorption isotherms of untreated K10 showed an increase in the adsorption with the increase of relative pressure (Fig. 4). The plot did not show a plateau at high pressure, which is characteristic of solids with a laminar structure [24, 33]. The desorption curve showed a hysteresis loop, indicating the possible presence of mesopores, which was verified in the BJH plot. The surface area determined by BET model was of 267.5 $m^2\ g^{-1}$. After the acid treatment, the adsorption isotherm showed a similar shape but lower surface area (184.7 $m^2\ g^{-1}$). The way organic molecules are adsorbed in a solid is reflected in its textural characteristics. Changes on the surface properties and morphology of the clay mineral after immobilization of organic compounds are rarely studied. Therefore, the analysis of textural characteristics was carried out for the samples containing each amino acid.

XRD study of samples containing amino acids

Once the amino acids were incorporated into the clay; the reflection corresponding to the interlayer space became more noticeable and shifted to other 2θ values, depending on the concentration and type of the amino acid. Figure 5 shows the XRD patterns of montmorillonite intercalated with aspartic acid, glutamic acid, and cysteine after the contact with amino acid solutions at two different concentrations. In the case of aspartic acid inclusion, a reflection around 6° of 2θ was observed at the low concentration, which corresponded to a *d*-spacing of 1.47 nm (Fig. 5a). When the amount of aspartic acid was increased to 100 mmol L^{-1} in the aqueous solution in contact with the solid, the XRD patterns showed a broad peak with a gradual increase to low angles, which indicated a maximum expansion of the interlayer space to values above 3.5 nm (Fig. 5d). In samples containing glutamic acid, the basal spacing was not clearly observed at the low concentration, although there was a barely distinguishable peak at d_{001} of 1.50 nm (Fig. 5b). At the higher concentration of this amino acid, the basal spacing was more evident with an expansion of 1.66 nm (Fig. 5e). The K10 clay containing cysteine showed similar XRD patterns at low and high concentrations, although a shoulder was distinguishable at the high concentration, observed at 5.3° of 2θ (1.66 nm) (Fig. 5c, f). It has been reported that the variation of basal spacing of samples containing organic compounds depends on the arrangement of molecules in the *d*-spacing, which value increases according to their orientation (d_{001} in: monolayer < bilayers < pseudotrimolecular layers < paraffin-type arrangements) [9]. The changes observed in the XRD pattern in the *d* spacing values suggested that the organic molecules were incorporated in different configurations between clay unit layers,

depending on the concentration and type of the amino acid. In the case of aspartic and glutamic acid, the decrease in the d_{001} value was produced when a minimal amount of organic molecules had occupied the interlayer space, removing water and suggesting a lateral monolayer arrangement of molecules [28]. When the concentration of amino acid was higher in the aqueous solution, a larger surface was covered by biomolecules, and the adsorption took place in a different conformation (probably paraffin-type) or forming multilayer in the basal space, producing an increase in the d_{001} value. On the other hand, samples containing cysteine showed similarity in their XRD patterns at both concentrations, which can be due to the fact that the molecules were only adsorbed in a single configuration. In this case, the d_{001} space was noticeably increased, which might be due to the fact that adsorption occurred either in a multilayer or a paraffin-type conformation.

FT-IR analysis of samples containing amino acids

In order to better understand the interaction between the amino acids studied here (aspartic acid, glutamic acid and cysteine) and the K10 surface, IR spectroscopy was used. Figure 6 shows the FT-IR spectra of K10 containing each amino acid at both concentrations. The main vibration bands from the amino acids were not distinguishable as they overlapped with the signals from the clay vibrations. Even though, FTIR spectra showed a band at 1,387 cm^{-1} from the symmetric vibration of the carboxylate ion in K10 containing the amino acid at the lower concentration (Fig. 6a–c). This band was more distinguishable in glutamic acid samples and less in solids containing cysteine, which might be due to the fact that cysteine has only one carboxylic group in its structure, while both the glutamic and aspartic acids have two. The asymmetric stretching mode of the C=O group (at 1,650 cm^{-1}) was not observed because either the carboxylic groups had charge or the signal overlapped with the clay bands [12, 34, 35]. When the amount of amino acid was increased to 100 mmol L^{-1} in the solution in contact with the K10 powder (Fig. 6d–f), the peak at 1,387 cm^{-1} vanished in the samples containing glutamic acid, and was hardly observed in the aspartic acid and cysteine samples, which shifted to 1,396 cm^{-1}. On the other hand, two broad bands emerged at the 1,407 and 1,528 cm^{-1} frequencies for K10-Glu-100. The first signal was due to the symmetric vibration of the carboxylate group, while the second one was assigned to the deformation vibration of the $-NH_3^+$ species. The samples containing aspartic acid and cysteine did not show noticeably these two bands, since these molecules were probably anchored in different conformations, or the amount of them on the surface was lower than in the case of glutamic acid. According to the diagram of species abundance (Fig. 7), the amino acids were completely deprotonated in the carboxylic groups during the sorption process in the clay, while the amino group was protonated. Therefore, $-COO^-$ groups remained unprotonated upon adsorption, and weak interaction took place between these groups and the solid surface. In addition, the organic molecule might also anchor to the clay surface through amino group interactions. FTIR showed mainly the carboxylate band (v_{sym} 1,386 cm^{-1}) at the low concentration of amino acid solutions, but this signal was shifted to 1,407 cm^{-1} once the amino acid concentration had increased in the initial solution. Although the carboxylate group can act as an uncoordinated anion ("ionic" form), as a monodentate or bidentate chelating ligand, or as a bridge bidentate group, the position of this $\nu(COO^-)$ band for amino acid metal complexes in the solid state is influenced not only by the direct coordination to a metal ion, but also by hydrogen bonding with water of crystallization, or some other intermolecular interaction with neighboring molecules [36]. In the same way, the amino group might be interacted with either hydroxyl groups of clay surface or hydrogen of neighboring molecules such as water or adsorbed amino acids. Observations made by other researchers have suggested that the adsorption of carboxylic acid on inorganic solids was carried out through a bidentate bond of carboxylate rather than a monodentate bond [6]. Therefore, it

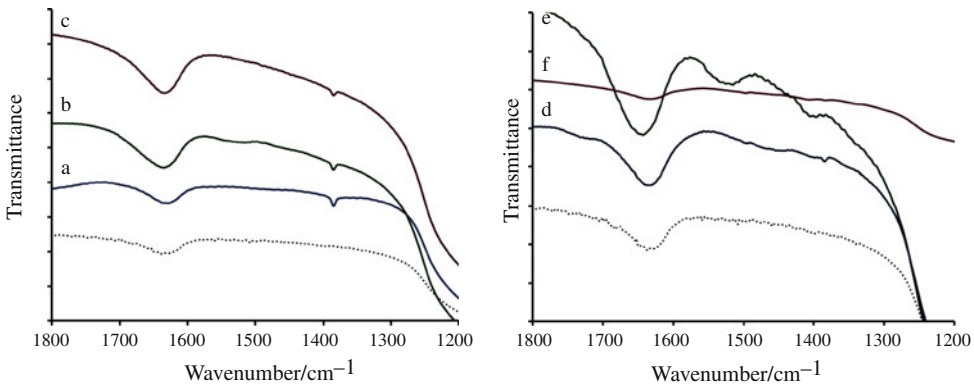

Fig. 6 FTIR spectra of K10 containing amino acids. *a* K10-Asp-1. *b* K10-Glu-1. *c* K10-Cys-1. *d* K10-Asp-100. *e* K10-Glu-100. *f* K10-Cys-100. The *dotted line* corresponds to acid-activated K10

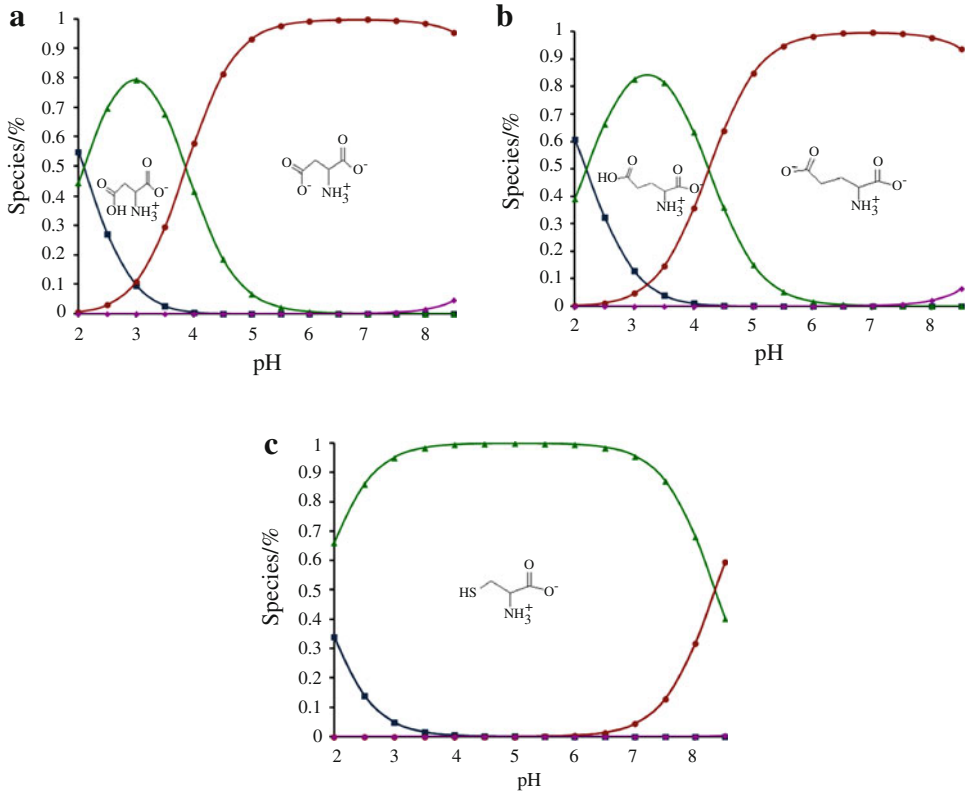

Fig. 7 Relative abundance of amino acid species in water at 25 °C and 1 bar, in function of pH. **a** Aspartic acid. **b** Glutamic acid. **c** Cysteine

was reasonable to assume that cysteine, aspartic, and glutamic acids were chiefly adsorbed to clay surface through interaction with the carboxylate group, but with a significant contribution from the amino group to the stability of the organic compound on solid particles. Even though it is very difficult to determine the mechanism of sorption, the FTIR analysis suggested that at the low concentration of the initial solution, the amino acid molecules were anchored to the clay surface in a specific way, while at the high concentration the organic molecule acquired different conformations, where the type and structure of the amino acid were decisive in the conformation, and amount of molecules adsorbed on the clay.

Thermoanalytical study of samples containing amino acids

Once the amino acids were incorporated into the clay structure; some changes were observed in the thermal behavior of samples. In the case of aspartic acid inclusion, the K10-Asp-1 showed a mass loss similar to observed in K10 samples (Fig. 8a). At low temperatures, the evaporation of both water and weakly bonded organic molecules occurred; the percentage of lost mass was about 3.05 % from 30 to 100 °C, and total mass loss of 3.7 % was observed from 30 to 200 °C. The difference of mass loss (from 30 to 200 °C) compared to K10 indicated that the aspartic acid molecules had occupied adsorption sites occupied initially by water molecules. In addition, the solid surface was not completely covered by organic molecules; instead, the clay probably contained both the water and aspartic acid molecules, and the amino acid was bonded to the surface more strongly than the water was. Therefore, during the annealing from 30 to 200 °C, water molecules were released, while the aspartic acid molecules remained on the solid. A mass loss of 2.94 % was observed from 200 to 500 °C, a slightly higher value than that observed in initial K10 sample. In this temperature range, the remaining aspartic acid was desorbed along with some water molecules. According to the DTG plot, the mass loss showed two maxima at 215 and 405 °C (Fig. 9a). It has been reported that aspartic acid bonded to a solid surface can be decomposed by a thermal procedure, producing NH_3 in the temperature range of 250 and 320 °C [13]. Taking into account the above reference, the decomposition of aspartic acid can supposed, in addition to the desorption processes from 200 to 500 °C. In the third stage of the TG curve (500–800 °C), the mass loss was about 1.03 %. Yuan et al. [13] again reported that reactions occurring at higher temperatures corresponded to the further decomposition of the guest species as well as the dehydroxylation process, producing H_2O, CO_2, and C_2H_4. Therefore, in this study, the mass loss from 500 to 800 °C was due to decomposition and dehydroxylation processes.

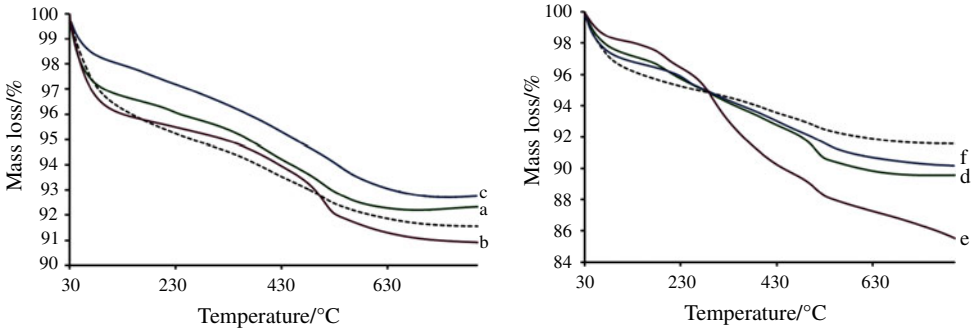

Fig. 8 Thermogravimetric analysis of K10 containing amino acids. *a* K10-Asp-1. *b* K10-Glu-1. *c* K10-Cys-1. *d* K10-Asp-100. *e* K10-Glu-100. *f* K10-Cys-100. The *dotted line* corresponds to acid-activated K10

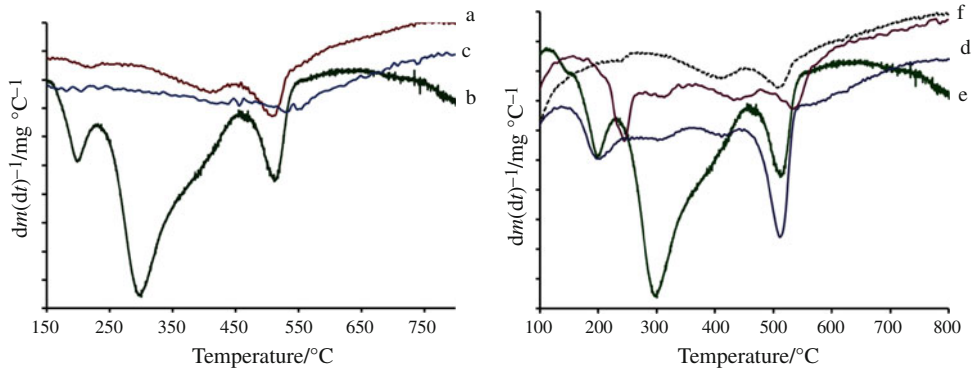

Fig. 9 DTG plots of K10 containing amino acids. *a* K10-Asp-1. *b* K10-Glu-1. *c* K10-Cys-1. *d* K10-Asp-100. *e* K10-Glu-100. *f* K10-Cys-100. The *dotted line* corresponds to acid-activated K10

When the aspartic acid amount was increased on the K10 surface, the TG curve showed the mass loss at different stage (Fig. 8d). A mass loss of 2.51 % was observed from 30 to 100 °C, and of 0.5 % from 100 to 150 °C. In this temperature range, the amount of released molecules was lower than in K10 and K10-Asp-1. This is due to the fact that most of the organic molecules were covering the surface and were strongly bonded to the adsorption sites of clay; therefore, less amount of molecules were desorbed at low temperatures. The molecules desorbed at low temperatures can mainly be of water. The DTG curve showed that most of the mass was lost at 196 °C (Fig. 9d). Above 200 °C, the solid began to lose mass gradually at a percentage higher than that of the initial K10. This mass loss was due to the removal of aspartic acid molecules from every adsorption site, such as the interlayer space, the surface, the edge, and interchangeable cations. These processes were carried out from 200 to 500 °C with a net mass loss of 5.86 %. Moreover, the highest mass loss in this temperature range was observed at 305 and 405 °C. In accordance with the comments made previously, the aspartic acid decomposition can take place during the annealing within this temperature range; accordingly, the decrease of mass by the decomposition reaction (at 305 °C) was more noticeable on a surface covered by a large amount of organic molecules. The K10-Asp-100 samples showed a total mass loss of 10.43 % from 30 to 840 °C. The DTG curve of K10-Asp-1 depicted the mass loss with three maxima at 215, 405, and 504 °C, while the K10-Asp-100 sample showed four maxima at 196, 305, 405, and 510 °C (Fig. 9a, d). The shift of points at maximum temperatures and the emergence of a new point can be due to the aspartic molecules being adsorbed in different conformations as well as to the higher interaction between neighboring organic molecules.

A mass loss of 9.08 % was observed in K10-Glu-1 with annealing up to 800 °C (Fig. 8b). These processes were carried out in different stages (Fig. 9b). The first took place from 30 to 100 °C corresponding to desorption of molecules weakly bonded to the surface, with a mass loss of 3.69 %. In this range, desorption of either water or glutamic acid molecules could have occurred. Little amount of mass of 0.67 % was removed with heating from 100 to 200 °C, attributed to the elimination of molecules anchored more strongly to the surface. The TG curve showed a gradual mass loss above 200 °C. This occurred mainly in two stages between 200 and 600 °C, with noticeable maxima at 295 and 504 °C (Fig. 9b). The processes occurring in this temperature range were probably due to the removal and decomposition of amino acid molecules. The total mass loss of K10-Glu-1 samples was slightly higher than that of aspartic acid which was an indicator that the glutamic molecules had more affinity to the activated-K10 surface. When the amount of glutamic acid was increased (K10-Glu-100), the larger amount of organic molecules was on the surface, occupying sites that were initially occupied by water. In these samples, a mass loss of 1.77 % was observed from 30 to 100 °C (Fig. 8e). The

glutamic acid molecules were bonded more strongly to the surface than the water molecules; therefore, they were not eliminated at low temperatures, and a low percentage of mass loss was observed. From this point, a gradual mass loss was observed during the sample annealing up to 850 °C; the processes occurred in different stages with maxima at 147, 194, 294, 495, and 504 °C (Fig. 9e). The thermal behavior of glutamic acid anchored on the clay surface could be explained by many reactions such as desorption, decomposition, and transformations. Initially, it could be assumed that decomposition occurred between 200 and 500 °C, with some decomposition products remaining adsorbed on the surface to be later eliminated above 500 °C. Lambert et al. [35] have reported that at high concentrations of glutamic acid in an aqueous solution, the adsorbed molecules on silica served as nuclei for the formation of small glutamic acid crystallites, which showed condensation reactions forming nitrogen cyclic compounds such as imides. Taking this into account, we assume that the reaction observed at 147 °C could correspond to a lactam ring closure. In the same sense, the possibility of polycondensation reactions at higher temperature could yield polymers with large chains, which molecules were anchored more strongly in the K10 surface, making it difficult for them to be removal by thermal treatment. For this reason, constant mass loss was still observed at 800 °C, without a constant plateau in the TG plot. It was possible that part of the organic molecules was not completely evolved, and these compounds were converted to intercalated charcoal. The total mass loss was 15.83 % up to 800 °C, a higher value than of the K10 containing aspartic acid. This indicated that the K10 surface showed higher affinity for adsorbing glutamic acid molecules than aspartic acid molecules.

In the case of the adsorption of cysteine on acid-treated K10, a different thermal behavior was observed (Fig. 8c). At the low concentration, the cysteine showed poor affinity to the K10 surface where the thermal evolution was observed in many stages; therefore, the mass loss occurred progressively from 30 to 850 °C, where no noticeable maxima were detected in the DTG curve (Fig. 9c). These reactions were probably due to the desorption and the decomposition of amino acid molecules, with the processes occurring at higher temperatures than those observed with aspartic and glutamic acids. This indicated that cysteine molecules were bonded more strongly on the K10 surface than the other amino acids; therefore, a higher temperature was necessary to desorb them. The total mass loss was 7.25 % up to 800 °C, which was the lowest observed value of all the amino acids studied. With K10-Cys-100, the coverage of the solid surface by the amino acid changed; hence, the thermal behavior of samples was different, showing mass loss in various stages (Fig. 8f). The first one was observed between 30 and 200 °C, corresponding to the desorption of both water and amino acid with a mass loss of 3.76 %. Others occurred from 200 to 500 °C, where three maxima were observed at 241, 306, and 430 °C (Fig. 9f). The suggested reactions in these processes were the transformation, desorption, and decomposition of cysteine, with a mass loss of 4.18 % in this range. Finally, a maximum was observed at 527 °C, which could due to the complete removal of organic compounds with a mass loss of 1.89 %. Then, the solid mass remained almost constant up to 800 °C. Many studies have reported the interaction of cysteine with inorganic solids [37–39], suggesting the formation of complexes with metallic ions in different conformation. In the case of the interaction of alkaline and alkaline earth metal cations with cysteine molecules, there is a tridentate conformation with amino nitrogen, carbonyl oxygen, and thiol sulfur atoms. If the metal cation is exchanged in a solid such as clay, this can attach cysteine molecules through coordination bonds with carboxylate, amino and sulfur groups. These functional groups can also interact with several active sites in clays such as montmorillonite. Therefore, the thermal behavior of cysteine anchored to the clay surface is determined by the adsorption site as well as the conformation of adsorbed molecules, and this amino acid was probably bonded more strongly to acid-activated K10 than the aspartic and glutamic acids were, hence higher temperatures were observed for the desorption and decomposition reactions.

Analysis by nitrogen adsorption at 77 K of samples containing amino acids

Figure 10 shows the nitrogen adsorption isotherm of samples containing amino acids. A similar behavior was obtained during the nitrogen adsorption of these solids compared to the observed one in acid-treated K10, which indicated that the laminar structure was preserved after the inclusion of organic molecules. Nevertheless, the surface area values varied with the inclusion of amino acid in the solid. Table 1 shows the surface area calculated from BET models as well as the average pore size. A similar increase was observed in each sample containing amino acid at the low concentration (initial solution 1 mmol L^{-1}); nevertheless, once the solution concentration was increased to 100 mmol L^{-1}, the impregnated solid showed a decrease in the surface area. At the low concentration of initial solution, molecules of both the water and amino acid were anchored on the K10 surface. A dispersion of agglomerates was probably produced by the presence of organic compounds on the particle surfaces, increasing the surface area of the powder. On the other hand, at the higher concentration of amino acid in the solid, organic molecules occupied the space of both the surface and micro-pore

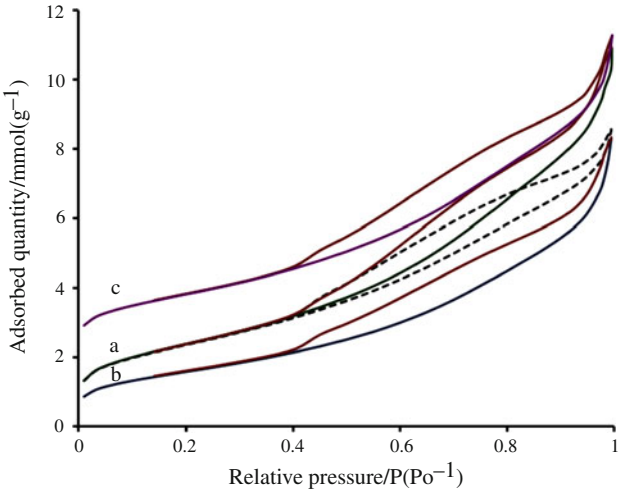

Fig. 10 Isotherm of nitrogen adsorption–desorption at 77 K of K10 containing amino acids. *a* K10-Asp-100. *b* K10-Glu-100. *c* K10-Cys-100. The *dotted line* corresponds to acid-activated K10

Table 1 Surface area measured by N_2 adsorption at 77 K and calculated by BET equation and pores size of acid-treated K10 samples containing amino acids

Sample	S_{BET}/m^2 g^{-1}	Pore size/nm
Acid-activated K10	184.7	5.72
K10-Asp-1	242.8	5.65
K10-Glu-1	223.4	6.72
K10-Cys-1	225.7	6.50
K10-Asp-100	193.8	7.21
K10-Glu-100	124.2	7.98
K10-Cys-100	199.6	6.96

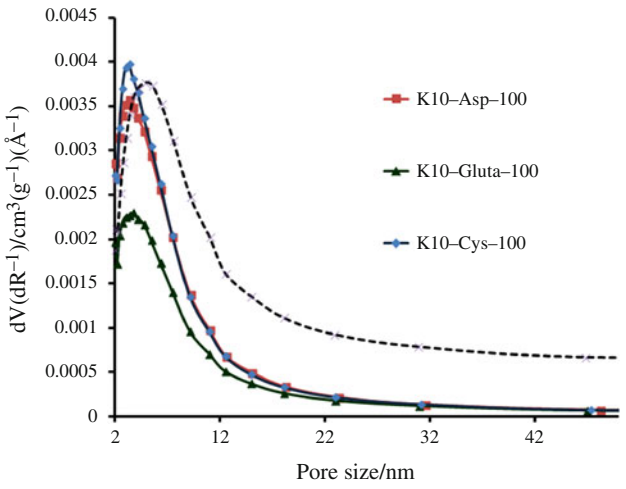

Fig. 11 BJH pore size distribution of K10 containing amino acids. The *dotted line* corresponds to acid-activated K10

cavities. In addition, when amino acid molecules were closer to each other on the surface, they could be due to stronger interaction and blocked pores. The BJH plots showed similar mesopore sizes distribution in K10 with the inclusion of each amino acid (Fig. 11), since the mesopore cavities were not modified with the amino acid incorporation; hence, the surface area changes were mainly due to either agglomerate dispersions or micropores obstruction. The reduction of surface area was the greatest in the samples of K10-Glu-100, a result that agrees with the observations made in the thermal analysis where higher mass loss was observed in these samples.

Conclusions

This study suggested that the adsorption of amino acids in acid-activated clay depended on the amino acid structure and the concentration of the aqueous solution in contact with the solid. At the low concentration of the initial solution, low affinity of the organic molecule with the material was observed, with poor coverage of the surface. X-ray analysis suggested that amino acid molecules were incorporated into the interlayer space, with the aspartic and glutamic acids retained in a monolayer arrangement, while the cysteine was hosted in a different orientation. The amino acid molecules were bonded strongly to the surface; therefore, greater mass loss was observed at higher temperatures during the thermal analysis. The cysteine was anchored more strongly than the aspartic acid and glutamic acid; hence, desorption and decomposition reactions were observed at higher temperatures for cysteine. The increase of the amino acid concentration in the solution produced changes in the *d*-spacing which was due to the different arrangements of organic compounds in the galleries of the layered silicates. Furthermore, the high concentration of these organic compounds in the initial solution in contact with the activated clay produced higher coverage of the surface. The acid-activated K10 showed a higher capacity to retain glutamic acid molecules than the others; for that reason, the samples containing this amino acid showed the greatest mass loss up to 800 °C. Infrared analyses of clay containing the amino acid showed bands corresponding to the carboxylate and protonated amino group, indicating that cysteine, aspartic, and glutamic acids were chiefly adsorbed through interaction with these functional groups. In addition, the textural characteristics of the powder were altered with the incorporation of amino acid molecules, suggesting agglomerate dispersion at the low concentration of the guest substance, while at the high concentration, the blocking of pores was assumed.

Acknowledgements This study has been financed by the University of Guanajuato through of DAIP office (Direccion de Apoyo a la Investigacion y el Posgrado). We acknowledge to Esthela Ramos and Cesar Contreras for their constructive comments about the manuscript. The authors also thank Martin Rodriguez Garcia for the figure edition in the manuscript.

References

1. Lopes I, Piao L, Stievano L, Lambert JF. Adsorption of amino acids on oxide supports: a solid-state NMR study of glycine adsorption on silica and alumina. J Phys Chem C. 2009;113:18163–72.
2. Trudeau TG, Hore DK. Hydrophobic amino acid adsorption on surface of varying wettability. Langmuir. 2010;26:11095–102.
3. Noren K, Loring JS, Persson P. Adsorption of alpha amino acids at the water/goethite interface. J Colloid Interface Sci. 2008;319:416–28.
4. Zaia DMA. A review of adsorption of amino acid on minerals Was it important for origin of life? Amino Acid. 2004;27:113–8.
5. Benetoli LOB, de Souza CMD, da Silva KL, de Souza Jr IG, de Santana E, Paesano A Jr, da Costa ACS, Zai TBV, Zai DAM. Amino acid interaction with and adsorption on clays: FTIR and Mösbauer spectroscopy and X-ray diffractometry investigation. Orig Life Evol Biospheres. 2007;37:479–93.
6. Giacomelli CE, Avena MJ, De Pauli CP. Aspartic acid adsorption onto TiO_2 particles surface, experimental data and model calculations. Langmuir. 1995;11:3483–90.
7. Wang X-Ch, Lee C. Adsorption and desorption of aliphatic amines, amino acid and acetate by clay minerals and marine sediments. Marine Chem. 1993;44:1–23.
8. Wedyan M, Preston MR. Isomers-selective adsorption of amino acids by components of natural sediments. Environ Sci Technol. 2005;39:2115–9.
9. de Paiva LB, Morales AR, Valenzuela-Díaz FR. Organoclays: properties, preparation and applications. Appl Clay Sci. 2008;42:8–24.
10. Kooli F. Exfoliation properties of acid-activated montmorillonite and their resulting organoclay. Langmuir. 2009;25:724–30.
11. Mallakpour S, Dinari M. Preparation, characterization, and thermal properties of organoclay hybrids based on trifunctional natural amino acids. J Therm Anal Calorim. 2013;111:611–8.
12. Wei M, Guo J, Shi Z, Yuan Q, Pu M, Rao G, Duan X. Preparation and characterization of L-cystine and L-cysteine intercalated layered double hydroxides. J Mater Sci. 2007;42:2684–9.
13. Yuan Q, Wei M, Evans DG, Duan X. Preparation and investigation of thermolysis of L-aspartic intercalated layered double hydroxide. J Phys Chem B. 2004;108:12381–7.
14. Zaia DAM. Adsorption of amino acids and nucleic acid bases onto minerals: a few suggestions for prebiotic chemistry experiments. Int J Astrobiol. 2012;11:229–34.
15. Basiuk VA, Gromovoy TY. Comparative study of amino acid adsorption on bare and octadecyl silica from water using high performance liquid chromatography. Colloids Surf A. 1996;118:127–40.
16. Lambert JF. Adsorption and polymerization of amino acids on minerals surface: a review. Orig Life Evol Biospheres. 2008;38:211–42.
17. Kitadai N, Yokoyama T, Nakashima S. ATR-IR spectroscopy study of L-lysine adsorption on amorphous silica. J Colloid Interface Sci. 2009;329:31–7.
18. Kitadai N, Yokoyama T, Nakashima S. In situ ATR-IR investigation of L-lysine adsorption on montmorillonite. J Colloid Interface Sci. 2009;338:395–401.
19. Meunier A. Clays. 1st ed. Berlin: Springer-Verlag; 2005.
20. Bhattacharga KG, Gupta SS. Adsorption of a few heavy metals on natural and modified kaolinite and montmorillonite: a review. Adv Colloid Interface. 2008;140:114–31.
21. Brown DR, Rhodes CN. Bronsted and Lewis acid catalysis with ion-exchanged clays. Catal Lett. 1997;45:35–40.
22. Chitnis SR, Sharma MM. Industrial applications of acid-treated clays as catalysts. React Funct Polym. 1997;32:93–115.
23. Pardhakar A, Cuadros J, Sephton MA, Dubbin W, Coles BJ, Weiss D. Adsorption of L-lysine on montmorillonite. Colloid Surf A. 2007;307:142–9.
24. Gregg SJ, Sing KSW. Adsorption, surface area and porosity. 2nd ed. London: Academic Press; 1980.
25. Bhowmik HHP, Zhao B, Hamon MA, Itkis ME, Haddon RC. Determination of the acidic sites of purified single-walled carbon nanotubes by acid-base titration. Chem Phys Lett. 2001;345:25–8.
26. Lopez-Ramon MV, Stoeckli F, Moreno-Castilla C, Carrasco-Marin F. On the characterization of acidic and basic surface sites on carbons by various techniques. Carbon. 1999;37:1215–21.
27. Fukushima Y. X-ray diffraction study of aqueous montmorillonite emulsions. Clays Clay Miner. 1984;32:320–6.
28. Liu H, Yuan P, Liu D, Tan D, He H, Zhu J. Effect of solid acidity of clay minerals on the thermal decomposition of 12-aminolauric acid. J Therm Anal Calorim. 2013;114(1):125–30. doi:10.1007/s10973-012-2887-0.
29. Madejová J. FTIR techniques in clay mineral studies. Vib Spectrosc. 2003;31:1–10.
30. Ursu AV, Jinescu G, Gros F, Nistor ID, Miron ND, Lisa G, Silion M, Djelveh G, Azzouz A. Thermal and chemical stability of romanian bentonite. J Therm Anal Calorim. 2011;106:965–71.
31. Balek V, Benes M, Malek Z, Matuschel G, Kettrup A, Yariv S. Emanation thermal analysis study of Na-montmorillonite and montmorillonite saturated with various cations. J Therm Anal Calorim. 2006;83:617–23.
32. Fajnor VS, Jesenák K. Differential thermal analysis of montmorillonite. J Therm Anal. 1996;46:489–93.
33. Mendioroz S, Pajares JA. Texture evolution of montmorillonite under progressive acid treatment: change from H3 to H2 type of hysteresis. Langmuir. 1987;3:676–81.
34. Vierira AP, Berndt G, de Souza-Junior IG, Di Mauro E, Paesano A Jr, de Santana H, da Costa ACS, Zaia CTBV, Zaia DAM. Adsorption of cysteine on hematite, magnetite and ferrihydrite: FT-IR, Mössbauer, EPR spectroscopy and X-ray diffractometry studies. Amino Acids. 2011;40:205–14.
35. Bouchoucha M, Jaber M, Onfroy T, Lambert JF, Xue B. Glutamic acid adsorption and transformation on silica. J Phys Chem C. 2011;115:21813–25.
36. Jalilehvand F, Mah V, Leung BO, Mink J, Bernard GM, Hajba L. Cadmium cysteine complexes in the solid state: a multispectroscopy study. Inorg Chem. 2009;48:4219–30.
37. Shankar R, Kolandaivel P, Senthilkumar L. Interaction studies of cysteine with Li^+, Na^+, K^+, Be^{2+}, Mg^{2+} and Ca^{2+} metal cation complexes. J Phys Org Chem. 2011;24:553–67.
38. de Santana E, Paesano A Jr, da Costa ACS, di Mauro E, de Souza IG, Ivashita FF, de Souza CMD, Zaia CTBV, Zaia DAM. Cysteine, thiourea and thiocyanate interactions with clays: FT-IR, Mössbauer and EPR spectroscopy and X-ray diffractometry studies. Amino Acids. 2010;38:1089–99.
39. Malferrari D, Brigatti MF, Laurora A, Medici L, Pini S. Thermal behavior of Cu(II), Cd(II)-, and Hg(II)-exchanged montmorillonite complexed with cysteine. J Therm Anal Calorim. 2006;86:365–70.